

Emulation of the space radiation environment for materials testing and radiobiological experiments

Jeffrey C. Chancellor,^{1,*} Stephen Guetersloh,² Keith Cengel,³ John Ford,² and Helmut G. Katzgraber^{1,4,5}

¹Department of Physics and Astronomy, Texas A&M University, College Station, Texas 77843-4242, USA

²Texas A&M University, Department of Nuclear Engineering, College Station, 77843-4242, USA

³University of Pennsylvania, Perlmutter School of Medicine, Philadelphia, USA

⁴IQB Information Technologies (IQBit), Vancouver, British Columbia, Canada V6B 4W4

⁵Santa Fe Institute, 1399 Hyde Park Road, Santa Fe, New Mexico 87501 USA

(Dated: June 12, 2017)

Radiobiology studies on the effects of galactic cosmic ray radiation utilize mono-energetic single-ion particle beams, where the projected doses for exploration missions are given using highly-acute exposures. This methodology does not replicate the multi-ion species and energies found in the space radiation environment, nor does it reflect the low dose rate found in interplanetary space. In radiation biology studies, as well as in the assessment of health risk to astronaut crews, the differences in the biological effectiveness of different ions is primarily attributed to differences in the linear energy transfer of the radiation spectrum. Here we show that the linear energy transfer spectrum of the intravehicular environment of, e.g., spaceflight vehicles can be accurately generated experimentally by perturbing the intrinsic properties of hydrogen-rich crystalline materials in order to instigate specific nuclear spallation and fragmentation processes when placed in an accelerated mono-energetic heavy ion beam. Modifications to the internal geometry and chemical composition of the materials allow for the shaping of the emerging field to specific spectra that closely resemble the intravehicular field. Our approach can also be utilized to emulate the external galactic cosmic ray field, the planetary surface spectrum (e.g., Mars), and the local radiation environment of orbiting satellites. This provides the first instance of a true ground-based analog for characterizing the effects of space radiation.

PACS numbers: 24.10.Lx, 02.50.Ey, 02.50.Ng, 02.70.Tt, 05.10.Ln, 05.60.Cd

I. INTRODUCTION

During spaceflight, astronauts are exposed to a variety of environmental stressors ranging from chemical and bacterial insults (resulting from the materials and occupants of the space vehicle) to microgravity and mixed fields of ionizing radiation. The space radiation environment is a complex combination of fast-moving ions derived from all atomic species found in the periodic table, with any meaningful abundance up to approximately Nickel (atomic number $Z = 28$). These ionized nuclei have sufficient energy to penetrate the spacecraft structure and cause deleterious biological damage to astronaut crews and other biological material, such as cell and tissue cultures [1, 2]. Furthermore, interaction with the spacecraft hull attenuates the energy of heavy charged particles and frequently causes their fragmentation into lighter, less energetic elements, changing the complexity and makeup of the *intravehicular* (IVA) radiation spectrum. Therefore, it is imperative to be able to emulate the space radiation environment both outside and within spacecrafts and, in particular, be able to quickly adjust to fast-paced materials research in space exploration. In this work we demonstrate an approach to emulate the space radiation environment in a laboratory setting. For simplicity, we focus on the IVA radiation spectrum measured on different spacecrafts. We emphasize, however, that our approach can be generalized to other radiation spectra and is therefore of wide applicability for general radiation studies, not just of biological material, but also for the deployment of e.g., shielding, electronics and

materials in a space environment.

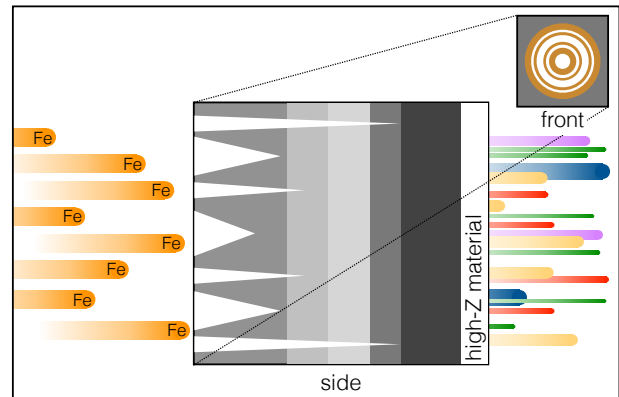


FIG. 1: Schematic of the moderator block designed to emulate specific space radiation spectra. A primary beam of ^{56}Fe (left) is selectively degraded with a carefully-designed moderator block to produce a desired distribution of energies and ions (represented by the colorful lines on the right-hand side). To preferentially enhance fragmentation and energy loss, cuts (white sections on the left-hand side) are performed in the moderator block made up of different materials (depicted by different shades of gray). Before the spallation products exit the moderator block, a high- Z material layer is added for scattering. The inset shows the circular beam spot, as well as the symmetric cuts made into the moderator block.

Recent studies have demonstrated that the biological response to space radiation is unique to a nonhomogeneous, multi-energetic dose distribution similar to the interplanetary space environment [3, 4]. It is therefore easy to conclude that previous radiobiological models and experiments utilizing

*Electronic address: jeff@chancellor.space

mono-energetic beams may not have fully characterized the biological responses or described the impact of space radiation on the health of vital tissues and organ systems. Currently, radiobiology studies on the effects of *galactic cosmic ray* (GCR) radiation utilize mono-energetic beams (e.g., Li, C, O, Si, Fe, etc.) at heavy-ion accelerators where the projected dose for an entire exploration class mission is given to animals using highly-acute, single ion exposures. This does not reflect the low dose rate found in interplanetary space, nor does it accurately replicate the multi-ion species and energies found in the GCR radiation environment that can cause multi-organ dose toxicity, inhibiting cell regrowth and tissue repair mechanisms [5].

There are many variables that contribute to uncertainties in the outcomes of space radiobiology studies: These include, first, the utilization of animal models with differing responses and sensitivity to radiation, second, epidemiology studies of human populations exposed to whole body irradiation at high doses limited to scenarios not found during space exploration missions (e.g., nuclear disasters), and third, simulating the spectrum of energies, ion species, doses, and dose rates found in the space radiation environment is a highly nontrivial endeavor [1]. The simultaneous experimental reproduction of *both* the dose rate and the ions found in the GCR spectrum is unlikely because of limits in current accelerator technologies. A reasonable goal would be to simulate the *linear energy transfer* (LET) distribution of the GCR environment. Although the LET is not uniquely related to biological response, it is an important metric that is utilized to determine radiation tissue damage. It remains the focus of many biological investigations and serves as the basis of radiation protection and risk assessment [5, 6]. In radiation biology studies, the differences in the *relative biological effectiveness* (RBE) of different ions are, in part, attributed to differences in the LET of the radiation [6]. Our model leverages available technologies to provide an enhancement to current ground-based analogs of the space radiation environment by reproducing the measured IVA LET spectrum.

Our goal is thus to numerically develop a target moderator block that can be easily constructed from materials with multiple layers of varying geometry to generate specific nuclear reactions and spallation products. The moderator block is designed so that the final field closely simulates the IVA LET spectrum measured on previous spaceflights. This target moderator block can be placed in front of, e.g., a 1GeV Iron (^{56}Fe) single-particle beam and nuclear spallation processes will create modest amounts of the desired fragments resulting in a complex mixed field of particle nuclei with different atomic numbers Z in the range $0 < Z \leq 26$ and LETs $\leq 500 \text{ keV}/\mu\text{m}$. The concept is shown in Fig. 1. Modifications to the internal geometry and chemical composition of the materials in the target moderator block allow for a shaping of the emulated IVA LET to specific spectra. The results from our numerical models are then compared to measurements of the IVA LET spectrum from the U.S. Space Shuttle orbiter during the Shuttle-MIR missions, the International Space Station (ISS), and NASA's new Orion Multi-Purpose Crew Vehicle (MPCV), clearly illustrating that the bespoke moderator blocks accurately replicate

the space radiation environment for ground-based radiobiology experiments.

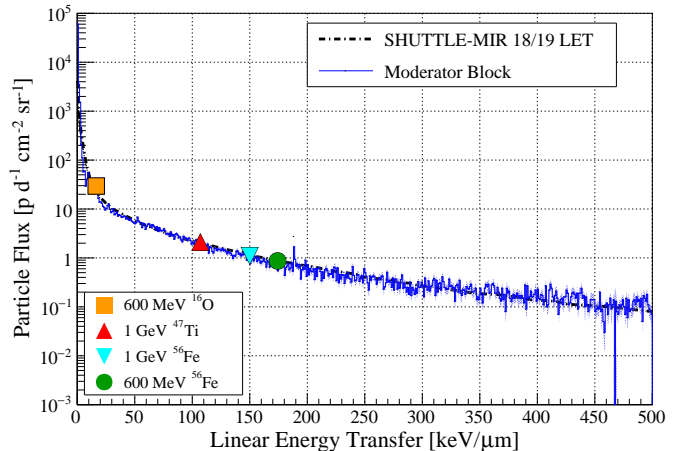


FIG. 2: Intravehicular particle flux versus the LET (measured in $\text{keV}/\mu\text{m}$) field from the Shuttle-Mir 18 and Shuttle-Mir 19 Missions measured by Badhwar *et al.* [7] (dashed line), as well as the results of our moderator block model simulation (blue solid line). The shading represents the statistical uncertainty in the model results. A close approximation of the measured LET spectrum is thus feasible for ground-based experiments. In addition, four single-ion exposures from current radiobiological experiments are shown (large symbols; see caption) to highlight the lack in breadth of energies in current radiobiological damage studies. In this and all other figures the particle flux is measured in particles per day, centimeter squared, steradian.

II. SELECTED CASE STUDIES

In what follows, we illustrate how the moderator blocks developed in this study can accurately reproduce the IVA LET for different space exploration missions. Details on the approach are outlined in subsequent sections. Note that the moderator block data are *simulated* using Monte Carlo methods. We do, however, show experimental validation of our simulations using experiments on homogeneous blocks.

A. Space Shuttle Orbiter

As a first example, the intravehicular LET spectrum during the Mir 18 and Mir 19 mission was chosen for initial validation of the model [7]. The Mir Space Station had an orbital inclination and flight altitude of 51.6° and approximately 200 nautical miles (370km). Beginning in March of 1995, NASA astronauts flew several long-duration missions on the Mir Space Station, returning to earth via the Space Shuttle. Badhwar *et al.* [7] measured the integrated LET spectrum that was directly attributed to GCR ions and their spallation progeny using tissue equivalent proportional counters (TEPC) and plastic nuclear track

detectors located at six different areas of the vehicle. Contributions from neutrons and non GCR particles (e.g., Van Allen Belt ions) were not considered in order to closely replicate their measured results.

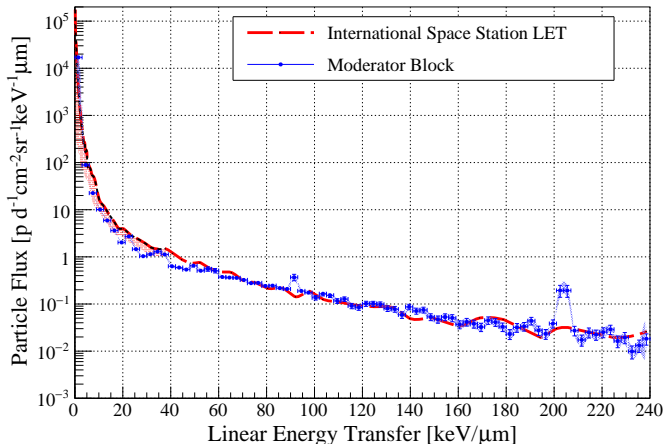


FIG. 3: Measured intravehicular LET field (per day) as measured on board of the ISS with the Timepix dosimeter (dashed line) compared to our moderator block model (blue solid line). The uncertainty in the numerical results is emphasized by the light blue shade. The spikes at LET approximately $90\text{keV}/\mu\text{m}$ and approximately $205\text{keV}/\mu\text{m}$ are due to an overabundance of energetic protons generated in the thicker layers of the modeled block. The red shaded area indicates an uncertainty in the low-energy measurements ($\text{LET} \leq 40\text{keV}/\mu\text{m}$). This is most likely due to secondary electrons stopping within the instrument’s silicon detector and resulting in an overestimation of approximately 10% to their LET values. Note that the original LET measurements were normalized per second. We have re-normalized to LET per day for consistency, as well as to display the estimated LET rate in units that are more relevant to radiation risk estimation for long-duration missions.

Figure 2 shows the LET (per day) measured during the Shuttle-Mir 18 and Shuttle-Mir 19 Missions [7] (black dashed line). The blue solid line represents the results of particle-transport simulations using the moderator block design developed in this work. A monoenergetic 1GeV Iron (^{56}Fe) beam passes the moderator block carefully designed to output the LET measured in orbit. The distribution of LET obtained from the beam-line simulation fits extremely well with the prediction for particles having a LET between $20\text{keV}/\mu\text{m}$ and $200\text{keV}/\mu\text{m}$ and with a reasonable fit for LET up to $500\text{keV}/\mu\text{m}$. The output is appropriately scaled to closely match the average daily LET rate measured. Note that the simulated target moderator block reproduces the spectrum over approximately six orders of magnitude. In comparison, Fig. 2 also shows individual mono-energetic ion beams (large symbols; see caption) currently used for radiobiological experiments. Clearly, these do not capture the richness of the measured IVA LET.

B. International Space Station

The International Space Station (ISS) was launched into orbit in 1998 and is still flying with an orbital inclination of 51.6° and an altitude of approximately 400km. The measured LET spectrum includes all charged particles (electrons, pions, heavy charged particles, etc.), however, like in the Badhwar *et al.* measurements for Mir [7], it excludes neutrons. Figure 3 shows the measured IVA LET spectrum from the ISS. LET measurements were taken using the *Timepix hybrid pixel detector* [8–10]. Again, the simulation of the designed moderator block matches the IVA spectrum of charged particles over many orders of magnitude.

The contribution of particles with low LET ($\leq 40\text{keV}/\mu\text{m}$) falls off much more slowly than what was seen for the Mir 18/19 measurements. This results in a moderator block with a far more complex geometry, including layers with thicknesses much greater than previously anticipated (e.g., larger than 50cm) that could generate the low- Z , high-energy particles needed to shape this portion of the LET distribution. The resulting spectrum closely matches the measured energies to a high degree of accuracy for continuous LET values of up to $240\text{keV}/\mu\text{m}$ over approximately seven orders of magnitude. The sharp peaks in the modeled LET spectra seen at $90\text{keV}/\mu\text{m}$ and $205\text{keV}/\mu\text{m}$ result from an overabundance of low-energy protons ($E \leq 2\text{MeV}$) generated in the thicker portion of the moderator block. These results indicate that modifications to the internal block geometry and material composition can successfully fit dose spectra for space vehicles with vastly different structure and shielding capabilities (i.e., the Space Shuttle versus the much larger International Space Station with thicker shielding).

C. Exploration Flight Test 1

The measurement results from NASA’s recent Exploration Flight Test (EFT-1) were recently made available and provided us with an opportunity to illustrate the robustness of our approach by demonstrating the ability to fit the IVA LET spectrum from a third space vehicle [11]. EFT-1 was the first flight of the new Orion Multi-Purpose Crew Vehicle (MPCV) that NASA will use for future interplanetary exploration missions. Although the MPCV had a much shorter flight duration of approximately four hours, the EFT-1 data are unique because of a high apogee on the second orbit that included traversal through the radiation-dense Van Allen Belts and briefly into the interplanetary radiation environment. Timepix-based radiation detectors were operational shortly after liftoff and collected data for the duration of the mission [12].

Similar to the Mir and ISS measurements, the EFT-1 flight data did not include measurements from noncharged particles (i.e., neutrons) which can provide a significant contribution to the total dose. We emphasize that our model can generate both thermal and fast spallation neutron products, however for better comparison with the measured data we did not include these in our LET spectrum. The EFT-1 flight data are shown in Fig. 4 along with the results of our model modified to accommodate

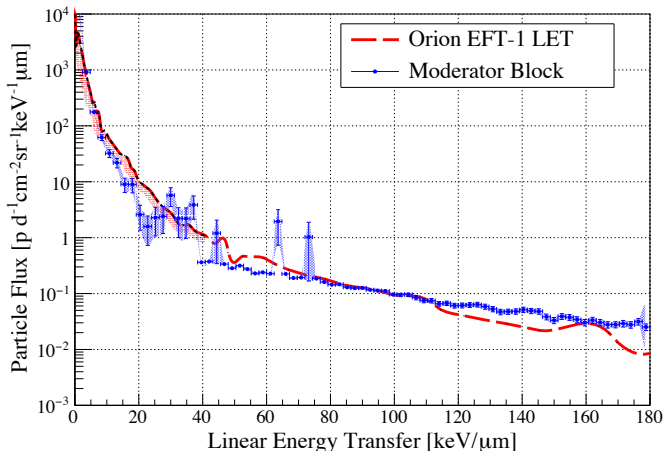


FIG. 4: LET field measured during the EFT-1 flight of NASA’s new Orion Multi-Purpose Crew Vehicle [11]. The EFT-1 mission lasted approximately four hours and included two orbits with a peak altitude of approximately 5800km. The LET was measured for the duration of the entire flight and averaged to LET per day. The exposure includes both interplanetary and Van Allen belt radiation fields. The mission is similar to the Apollo 4 mission of 1967, that validated the Apollo flight control system and heat shield at re-entry conditions planned for the return from lunar missions.

for the unique spectrum. Our results fit reasonably well with the flight measurements, however with visible fluctuations in the 30 — 80keV/ μm range with several sharp peaks at approximately 65keV/ μm and 73keV/ μm . This weakly corresponds to a smaller fluctuation found from 30 — 50keV/ μm in the measured data. It is not yet clear whether these are indicators of the true nature of the measured LET spectrum, or are simple statistical fluctuations resulting from the smaller measurement period of the EFT-1 flight. Moderator layers made of polymers as thick as 100cm are required to produce this LET spectrum. The sharp peaks at approximately 65keV/ μm and 73keV/ μm in our results are due to an overabundance of ions with charge $Z \leq 6$ in these 90cm and thicker layers. We note that in our models effort was made to use *few* hydrogen-rich materials (see Sec. III). The difficulty in reproducing the EFT-1 data may be an indication that other low- Z materials and metamaterials should be considered in future studies.

III. METHODS

Highly-charged heavy ions penetrate matter with an approximate straight path and gradually dissipate energy through multiple collisions with matter atoms and their electronic structure. The interaction of the highly-charged heavy ion with the atomic structure of a material results in one of two outcomes: Either the primary ion loses energy to the medium, or it generates smaller progeny nuclei that result from spallation processes. Both of these outcomes are influenced by the energy and charge of the primary ion, but are also strongly dependent on the properties of the material being targeted. The effec-

tiveness of a material to instigate energy loss attenuation and spallation typically increases with decreasing atomic number, with hydrogen being the most efficient.

A. Material Selection

The energy loss of a heavy charged particle is primarily associated with the many interactions with electrons and the effective stopping power of the material these ions are penetrating. The loss of energy can be approximated to high accuracy using the stopping power equation [13]:

$$\frac{dE}{dx} = \frac{4\pi e^4 Z_1^2 Z_2}{m_e \beta^2} \left[\ln \left(\frac{2m_e v^2}{I} \right) - \ln(1 - \beta^2) - \beta^2 - \frac{C}{Z_2} - \frac{\delta}{2} \right]. \quad (1)$$

Here, Z_1 and Z_2 are the charges of the primary ion and the medium being traversed, respectively, m_e electron mass density of the medium, and $\beta = v/c$ with v the velocity of the primary ion and c is the speed of light. Material-specific effects are described by the average ionizing potential of the medium I , the shell correction C/Z_2 , and the density effect δ . These have been validated with both theoretical and experimental results, see Refs. [14–16] for details. The stopping power is equivalent to the energy loss per unit path length of the primary ion, i.e., the LET,

$$\text{LET} \equiv dE/dx. \quad (2)$$

The LET quantifies how much energy is lost in a material and is typically given in units of keV/ μm for radiobiological quantification of damage. Note that there is also a probability that the heavy charged particle fragments into smaller, low-energy ions due to spallation processes that result from interactions with the nuclei in the material.

The contribution to Eq. (1) made by the density effect correction δ is only significant for particles with kinetic energies that exceeds their rest mass (i.e., energies larger than approximately 1GeV) [16–20]. This exceeds the energy of primary particles considered in this study and does not play a significant role in the material selection. C/Z_2 , provides a correction to the stopping power for ions with energies smaller or equal than 200MeV, where their velocity is equal to or less than the orbital velocity of the lattice electrons. This correction is most pronounced for ions with energies less than 10MeV that populate the higher LET spectrum (e.g., energies $\geq 100\text{keV}/\mu$). The average ionization potential I provides the largest opportunity to perturb the medium’s properties in order to instigate specific changes in the emerging particle spectra that more closely model the desired field. It describes how easily a target material can absorb the kinetic energy imparted from the projectile through electronic and vibrational excitation. Unlike the density and shell corrections, whose relative contribution to stopping is strongly dependent on the projectile’s energy and/or atomic charge, I is a characteristic measure of the target material only. It has no dependence on the properties of the projectile ion. Because the contribution of I to stopping is

logarithmic, small changes in its value do not produce major changes in the stopping cross section [15, 21, 22]. This provides an opportunity to make fine adjustments to the energies of the emerging particles by making perturbations around the measured values of the mean excitation potential for the material under considerations.

We choose hydrogen-rich materials for the moderator blocks. Spallation, and especially the energy loss spectrum for a heavy ion beam in a particular material is strongly dependent on the beam species, energy, and the properties of the target material being traversed. Polymers, meta-polymers, and hydrogenated materials are favorable materials because per unit mass, these hydrogenous materials cause higher fragmentation of high-energy heavy ions and stop more of the incident low-energy particles than other materials [15, 23] [see Eq. (1) and the explanation of the different terms above]. Thus, polymers are suitable candidate materials because they have a high hydrogen content and, as an added bonus, have sufficient tensile strength for machining [21, 24–27]. For example, polyethylene (CH_2) with two hydrogen atoms and one carbon atom per monomer is ideal for the design and construction of moderator blocks. The use of readily-available materials allows radiation researchers at different research centers — for example the European Space Agency — to generate reproducible results at any heavy-ion accelerators capable of providing 1GeV ^{56}Fe ions.

Predicting the resulting particle species, their multiplicity, and corresponding energies is not possible to any high degree of accuracy. To overcome the highly-stochastic results of primary fragmentation, our models vary the length of the interaction in the material to quantify what material(s) and geometric properties of the moderator block could best produce the desired range of ions and resulting energies.

B. Block Geometry

In any medium, there is a finite probability for secondary, tertiary, and higher-order generation of nuclear interactions that involve the primary ^{56}Fe ions. The energy loss of the primary and its progeny created by spallation also increase with depth, and this begins to counter the expected decrease in average LET caused by fragmentation. The LET of the primary nuclei and higher- Z fragments typically increase rapidly as the depth of the moderator block increases. As the primary slows and its energy decreases, the LET rises sharply at depths that are small compared to the mean free path for a nuclear interaction and the effects of energy loss outweigh those of fragmentation. Additionally, as the moderator's depth increases, the number of ions available to fragment into lighter ions is depleted by spallation events at shallower points in the target. At moderator depths much greater than the range of the incoming ^{56}Fe primary, the heavy charged fragments begin to slow and stop, and their contribution to the LET of the emerging field decreases. At great depths, the charged particle dose is due to high-energy, singly-charged particles such as protons, charged pions, He, etc., all of which have very long penetration depths in polymers (approximately 3 — 4m for a 1GeV proton in CH_2).

The length of travel through a medium can not only change

the number of desired lower- Z ions generated and the energy loss of the primary and secondary ions generated, but it can also affect nuclei yields by depleting the number of high- Z ions still needed. In order to generate the GCR spectrum, the moderator geometry and thickness need to balance the effects of energy loss and fragmentation. This is done by designing the moderator block geometry such that it replicates the attenuation function for a desired field of a given energy. Each channel or “cut” represents a separate path the primary ions can travel through the block, see Fig. 1. The diameter, length and material of each cut are chosen such to induce specific spallation and energy loss events of the primary ion. This provides a method to selectively induce specific fragmentation and energy losses that result in the emerging field having the desired distribution of emerging ions and energies.

A three-dimensional version of the moderator block is then recreated using combinatorial geometry for the PHITS Monte Carlo simulation. This includes accurate determinations of the width, length, and curvature of the various channels and cuts. The chemical composition and density specific to each of the moderator's layers also has to be specified for determining the material properties, such as atomic structure, ionization potential, electron shell configuration, etc.

C. Numerical Details

The simulations are performed using the Monte Carlo particle transport simulation software PHITS [28], in order to model particles traversing through thick absorbers and to approximate the desired LET spectrum. The correct fluence of particles required can be determined using data from, e.g., satellite measurements, intravehicular measurements during space missions, or from peer-reviewed models of the GCR spectrum [29]. PHITS features an event generator mode that produces a fully-correlated transport for all particles with energies up to 200GeV [28]. The software calculates the average energy loss and stopping power by using the charge density of the material and the momentum of the primary particle by tracking the fluctuations of energy loss and angular deviation. PHITS utilizes the SPAR code for simulating ionization processes of the charge particles and the average stopping power dE/dx [30, 31]. PHITS has been previously compared to experimental cross-section data using similar energies and materials. Zeitlin *et al.* [32, 33] showed for large detector acceptance angles, that there is good agreement between experimental beam-line measurements of fragmentation cross sections and the simulated outcomes that utilized PHITS to generate the expected progeny fragments and energy loss.

We have chosen PHITS mainly because the software can be run in parallel mode and thus take advantage of large-scale multi-core high-performance computing platforms. A full description of the capabilities of PHITS and the various nuclear models utilized in the code can be found in Ref. [28]. We have verified our results using other software packages and our results are independent of the software used within error bars (not shown) [34, 35].

A two-dimensional schematic of the moderator block model

used in the Monte Carlo simulation is shown in Fig. 1. The 1GeV ^{56}Fe primary beam is accelerated from the left, propagated through the moderator block and emerging along with progeny fragments generated during spallation reactions with the block materials. The field continues to the right where a scoring plane is located 1m from the moderator block face. Particle species, energy, and directional cosines are recorded for analysis and LET calculations. The LET values (in tissue) are then calculated using the stopping power formula described in Eq. (1). All particles are scored, including electrons, pions, neutrons, etc. However, only the charged particles were considered for the final LET spectrum.

The medium traversed by the particle field emerging from the moderator is assumed to be open air. For these simulations we chose the ambient environment measured in the beam house at the NASA Space Radiation Laboratory located at Brookhaven National Laboratory. This allows “air attenuation” of low-energy particles by allowing 1m of travel between the back plane of the moderator and the scoring plane. Additionally, this simulates the moderator placed in a beam-line with the hardware, tissue, or biological samples located 1m down the beam line.

D. Neutrons

Neutrons and other noncharged particles were not included in our LET calculations primarily because they were not included in the flight measurement data and, in this work, all effort was made to accurately reproduce these data sets. Spallation neutrons are typically present. However, they should not be included without reliable and accurate measurements from spaceflights – data that are currently unavailable. Such measurements are hard to perform. Charged particles move (mostly) along a straight path losing energy according to Eq. (1). Knowing their energy, ion type, and corresponding LET provides enough information to evaluate the biological impact as the charged particle propagates from the skin surface and through soft tissue. In contrast, neutron propagation is far more sporadic. During any interaction, a neutron may deposit only a small fraction, or even all of its energy into the medium. Therefore, we feel that an accurate measurement of the IVA neutron spectrum is needed, before the neutron contribution can be distinguished from the charged particle spectrum.

E. Statistical Error Analysis

Systematic errors are attributed to the many approximations required for a three-dimensional particle-transport Monte Carlo simulation and are, unfortunately, out of our control. The bootstrap method was utilized to determine the statistical stability of the results and minimize systematic biases in the outcomes [36]. Several discrepancies between the spectrum resulting from beam-line simulation still remain to be resolved. It is not yet known how well the target design reproduces the LET distribution for particles with LETs that have less than approximately $5\text{keV}/\mu\text{m}$. Based on past calculations, we predict that

any discrepancies may be resolved by adjusting the geometry and/or atomic composition of the proposed target moderators.

F. Direct Model Validation with Experimental Data

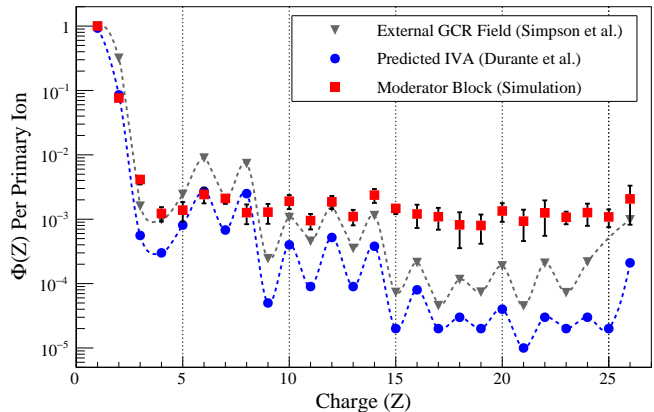


FIG. 5: Comparison of predicted charge distributions. The relative abundance of IVA ions in the exiting field created by the moderator block (red squares), as well as the results of Durante *et al.* [37] (blue circles) as a function of the atomic number Z . The lower- Z ions ($Z \leq 8$) that contribute to the majority of the entire spectrum closely match the predicted abundance. There is a close similarity in the distribution of ions for $Z \leq 14$. As Z increases up to ^{56}Fe ($Z = 26$), the charge distributions diverge similarly, but with the moderator block generating more heavy ions.

All models, to a certain degree, are unable to capture all features measured in experiments. Their utility depends on how accurately they can reproduce physical observations and measurements, as well as make predictions. Our primary hypothesis was to develop a model that recreated the IVA LET spectrum as measured in spaceflight vehicles. The stopping power, and thus the energy loss of charged particles transported through single-ion materials and most compounds has been exhaustively validated with experimental results [21, 24–27].

As an example, we analyze in more detail the Shuttle-Mir missions depicted in Fig. 2. The relative accuracy of the charge distribution resulting from the moderator block is shown in Fig. 5. These results provide initial evidence that we could, perhaps, with clever utilization of materials and geometry, match both the LET *and* the the charge distribution of the measured field. This would provide a true, ground-based analog of the space radiation environment. Our preliminary validation study will thus focus on the prediction accuracy of progeny fragments created by the highly stochastic spallation processes. Here we compare our moderator block model to experimental measurements of the fragmentation production of 1GeV ^{56}Fe ions incident on several different targets. The target materials include pseudo-thin and thick hydrogen-rich compound materials (CH_2), Lead (^{208}Pb), and Aluminum (^{26}Al), which are commonly found in the structure of space vehicles. The fragmentation and particle multiplicity are reproduced using

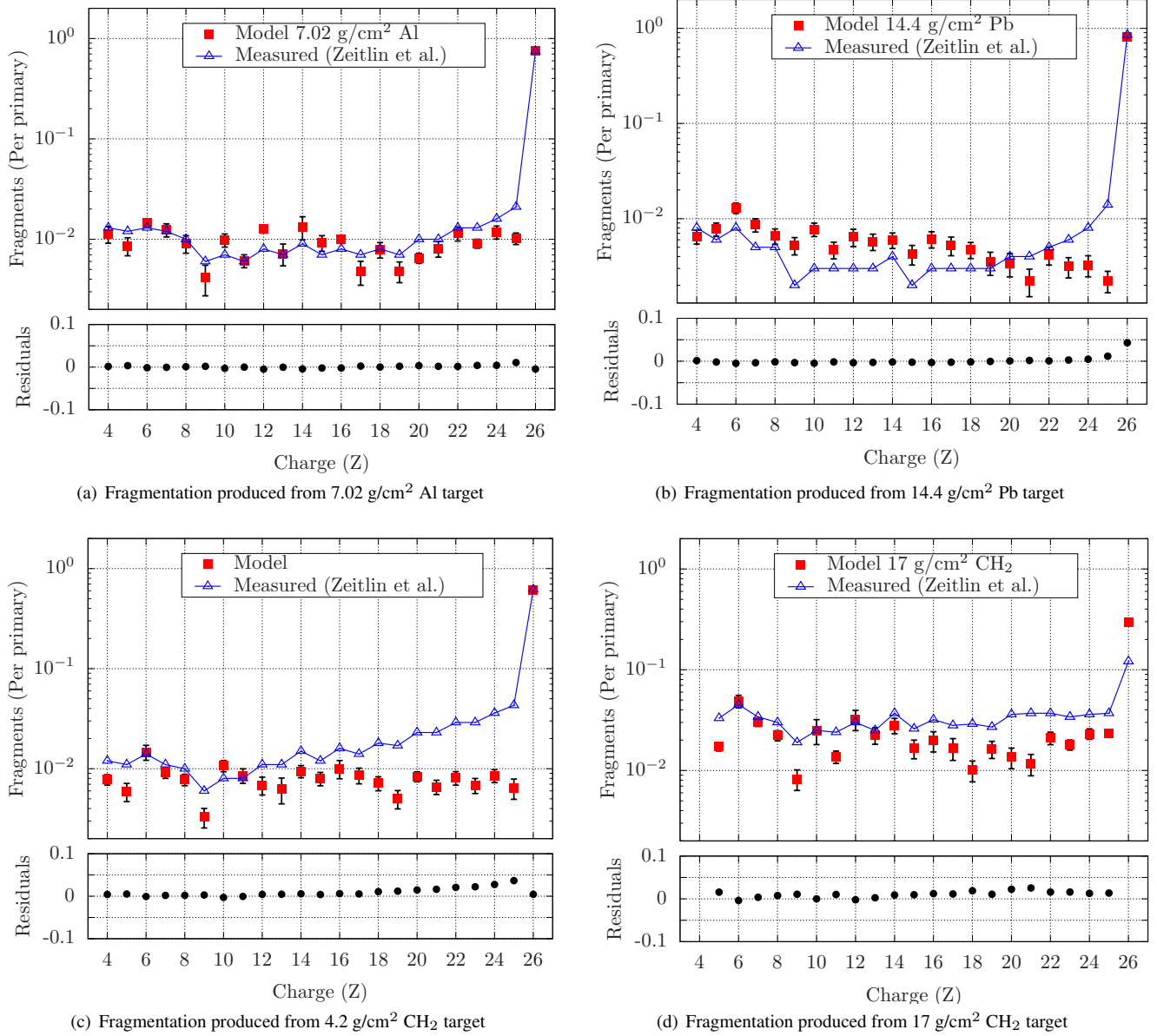


FIG. 6: Comparison of charge multiplicity in mono-ion and compound targets. The relative abundance of fragment ions per primary in the exiting field created by the moderator block (red squares), as well as the measurement results of Zeitlin *et al.* [23] (blue circles) as a function of the atomic number Z . For each case, there is a close agreement in the surviving ^{56}Fe primaries with the measured fraction of surviving projectiles measured by Zeitlin *et al.* This provides good initial indication that our model is very capable of accurately replicating the mechanisms of charge-changing interactions. Additionally, there is a visible preference for even charged progeny, as demonstrated by Zeitlin and previous experiments [33, 38]. In the mono-species target blocks [panels (a) and (b)] there is very good agreement with the measured charge distribution, including the expected enhancement of $Z = 14$ (Si) and suppression of $Z = 9$ (F). Panel (c): In the (thin) CH₂ target, the progeny ions created in fragmentation reactions closely match the predicted abundance up to approximately $Z \leq 16$. There is a very close match with the amount of surviving primary ions, ^{56}Fe . There is a close similarity in the distribution of ions for $Z \leq 17$. As Z increases up to ^{56}Fe ($Z = 26$), the charge distributions diverge similarly, but with the the moderator block generating less heavy ions to within one order of magnitude. Panel (d): Similar to the thin CH₂ target, the progeny ions created in fragmentation reactions closely match the predicted abundance up to approximately $Z \leq 14$, with the amount of surviving ^{56}Fe primary ions slightly higher than measured. There still remains a close similarity in the distribution of ions for $Z \geq 15$ up to ^{56}Fe ($Z = 26$), where the charge distributions diverge (to within one order of magnitude) with the the moderator block generating less of the heavier ions.

our moderator block model and compared with the published results of Zeitlin *et al.* [23, 32, 33, 39].

Figures 6(a) – 6(d) demonstrate that our model provides a close reproduction of the charge distribution measurements

for each of the target blocks. The fluence of surviving ^{56}Fe primaries agrees closely with the measured fraction of surviving projectiles measured, providing an initial demonstration of the model's accuracy in replicating the mechanisms of charge-changing interactions. In each case, the odd-even effect is clearly visible, with a slight preferential enhancement of even charge fragments. Knott *et al.* first demonstrated this effect for projectiles with isospin $T_z = 0$ [38], but Zeitlin *et al.* showed that there was still a subtle, but pronounced odd-even trend with 1 GeV ^{56}Fe projectiles ($T_z = -2$) [40].

Previous studies have shown that the closed $d_{5/2}$ Si sub-shell should lead to an enhancement of $Z = 14$ (Si) fragments. This is seen in Figs. 6(a), 6(b), and 6(c), but is less subtle in Fig. 6(d). This trend is repeated in the measured suppression of $Z = 9$ (F). This is seen in the ^{26}Al , ^{208}Pb and thinner CH_2 target(s), but is less obvious in the thick CH_2 target block.

The measured fluence of progeny fragments is accurately replicated with our model to within approximately half an order of magnitude or less for each test case. We agree that there is still room for improvement. However, we are merely demonstrating a proof-of-principle design. In addition, compared to previous monoenergetic single-ion beam studies, our model represents a far more accurate emulation of the effects of space radiation. The trend for both single material blocks, ^{26}Al and ^{208}Pb , has good agreement for all charges $4 \leq Z \leq 26$. In the 4.2 g/cm^2 CH_2 target, there is good agreement for $4 \leq Z \leq 16$ with subsequent divergence for charges greater than $Z=17$. A similar trend is seen in the thick CH_2 target, Fig. 6(d), but with our model results diverging at $Z \approx 15$. Additionally, the survivability of the primary ^{56}Fe is underpredicted in the thicker CH_2 target block, but within an acceptable half-order of magnitude.

Summarizing, our model demonstrates that the intrinsic properties of hydrogen-rich crystalline materials can preferentially produce specific nuclear spallation and fragmentation processes when placed in an accelerated heavy-ion beam. The perturbation of their micro-structure can influence the material's capability to simultaneously generate the complex mix of LET, nuclei, and energies found in the GCR spectrum. Astrophysics models should demonstrate an agreement better than 10% with measured and observed data [38]. The underemphasis of $17 \leq Z \leq 25$ charges in Fig. 6(c) and $Z \geq 6$ charges in Fig. 6(d) is likely attributed to a weakness of the cross-section dynamics for charged particle transport where the normalization factors used in the interaction model(s) are less effective as fragment Z increases towards the charge of the projectile ion. These higher- Z fragments are produced in peripheral collisions that are very sensitive to the choice of allowed impact factors defined in the molecular dynamics, leading to interaction cross-sections that are hyper-responsive to the primary ion's energy and charge, target material(s), etc. Previous research studies that have demonstrated a preference for low- Z targets to generate low- Z fragments (e.g., $Z \lesssim 8$). In our study we observe an accurate replication of surviving primaries in both of the CH_2 target(s), but a noticeable divergence of progeny fragments created as Z increases. These results indicate further tuning of our model is needed, and perhaps the exploration of other target materials and meta-materials.

IV. APPLICATIONS & CLINICAL UTILITY

The clinical utility of models for predicting the dose-toxicity response to space radiation in astronauts is currently limited by radiobiology studies that utilize mono-energetic beams, e.g., Li, C, O, Si, and Fe at heavy-ion accelerators where the entire projected dose for an exploration-class mission is given to animals using high dose rate exposures. These single-ion, mono-energetic heavy-ion exposures reflect neither the low dose rate nor the complex energetic and ionic make up of GCR radiation, and *in vivo* experiments with such beams are unlikely to accurately model the potential multi-organ toxicity of GCR radiation [5].

Because simultaneously reproducing both the species abundance and energies of the GCR is unlikely in current experiments, a more reasonable goal is to simulate the LET distribution of the GCR spectrum. In radiation biology studies and the assessment of health risk to astronaut crews, the differences in the relative biological effectiveness (RBE) of different heavy ions are primarily attributed to differences in the LET spectra of the radiation [41]. While the specific ion species depositing dose may have biological significance, the LET distribution created by the intrinsic properties of these ion species is most critical when determining the biological response. Here, the LET serves as the basis of radiation protection and risk assessment in mixed radiation exposure scenarios [5, 41].

In addition to utilizing mono-energetic beams, currently radiation effects studies include exposing samples to a dose rate of approximately 200mSv/min. The NASA Space Radiation Laboratory lists the *maximum* spill rate for 1GeV Fe ions as approximately $5 \cdot 10^8$ ions per second. In this simulation, approximately $5 \cdot 10^8$ primary ions were used to match the integrated LET rate per day as measured by Badhwar *et al.* At this spill rate, our results can provide the equivalent daily dose rate every single second. When compared to a measured spectrum from the International Space Station, this would be an equivalent dose rate of 36mSv/min. In other words, 6.1 minutes of exposure at NASA's Space Radiation Laboratory (or any equivalent heavy-ion accelerator) would be equivalent to the projected exposure of an astronaut spending one year on board the ISS. In fact, the approximate integrated dose for a one-year mission on board the International Space Station (ISS) in a low-Earth orbit is approximately 200 – 250mSv, which is a factor of 6 decrease in the dose rate. Assuming a controlled reduction of the beam spill rate at NASA's Space Radiation Laboratory, it is very feasible to assume that a significantly lower dose-rate can be achieved. The results would be a ground-based analog for the space radiation environment that closely mimics the dose-rate, distribution of ion species, and the expected LET spectrum measured on previous spaceflight missions.

V. CONCLUSIONS

Our moderator block model demonstrates that the intrinsic properties of hydrogen-rich crystalline materials can preferentially produce specific nuclear spallation and fragmentation processes when placed in an accelerated heavy-ion beam. The

perturbation of their micro-structure can influence the materials capability to simultaneously generate the complex mix of nuclei and energies found in, e.g., the GCR spectrum. NASA is proposing a GCR simulator that will provide three to five consecutive mono-energetic heavy ions. Such an approach only provides a few LET data points (see Fig. 2) and lacks the generation of pions and neutrons that account for 15 – 20% of the dose [42]. Additionally, questions still remain on what order the ion species should be given since this can affect the outcomes of the experiment [43, 44]. Our approach provides a significantly more robust and accurate recreation of the space radiation environment by allowing for a continuous generation of ionizing radiation that matches the LET spectrum and dose rate of GCR for experiments with ground-based analogs. This is of paramount importance at the moment, where new expandable ISS modules using novel materials are being deployed. Current radiation testing on biological samples is even more accessible on orbit using the recently-launched Bigelow Expandable Activity Module (BEAM). Being able to recreate the

space radiation environment on Earth as we have demonstrated here, would significantly boost the development of space exploration while drastically cutting costs and reducing risks.

VI. ACKNOWLEDGMENTS

We would like to thank Nicole Stott and Eric Gignac for help with the graphics. J. C. C. would like to thank Nicolas Stoffle for the discussions about the ISS and EFT-1 LET measurement data, James Ziegler for reviewing the concept and theory, and Serena Aunon-Chancellor for the many proof-reads and valuable input. H. G. K. acknowledges support from the National Science Foundation (Grant No. DMR-1151387). The authors acknowledge the Texas Advanced Computing Center (TACC) at The University of Texas at Austin for providing HPC resources that have contributed to the research results reported within this paper.

-
- [1] J. C. Chancellor, G. B. Scott, and J. P. Sutton, *Space radiation: the number one risk to astronaut health beyond low earth orbit*, *Life* **4**, 491 (2014).
- [2] S. A. Walker, L. W. Townsend, and J. W. Norbury, *Heavy ion contributions to organ dose equivalent for the 1977 galactic cosmic ray spectrum*, *Adv. in Space Res.* **51**, 1792 (2013).
- [3] A. R. Kennedy, *Biological effects of space radiation and development of effective countermeasures*, *Life Sciences in Space Research* **1**, 1 (2014).
- [4] A. L. Romero-Weaver, X. S. Wan, E. S. Diffenderfer, L. Lin, and A. R. Kennedy, *Effect of SPE-like proton or photon radiation on the kinetics of mouse peripheral blood cells and radiation biological effectiveness determinations*, *Astrobiology* **13**, 570 (2014).
- [5] J. W. Wilson, R. C. Thibeault, F. A. Cucinotta, M. L. Shinn, M. H. Kim, R. Kiefer, and F. F. Badavi, *Issues in protection from galactic cosmic rays*, *Radiat. Environ. Biophys* **34**, 217 (1995).
- [6] ICRU, Tech. Rep. (1991).
- [7] G. D. Badhwar, W. Atwell, B. Cash, V. M. Petrov, Y. A. Akatov, I. V. Tchernykh, V. A. Shurshakov, and V. A. Arkhangelsky, *Radiation Environment on the Mir Orbital Station During Solar Minimum*, *Advanced Space Research* **2**, 501 (1998).
- [8] L. Pinsky, J. Chancellor, and D. Minthaka, in *Aerospace Conference, 2008 IEEE* (IEEE, 2008), p. 1.
- [9] N. Stoffle, L. Pinsky, M. Kroupa, S. Hoang, J. Idarraga, C. Amberboy, R. Rios, J. Hauss, J. Keller, A. Bahadori, et al., *Timepix-based radiation environment monitor measurements aboard the International Space Station*, *Nuclear Instruments and Methods in Physics Research Section A: Accelerators, Spectrometers, Detectors and Associated Equipment* **782**, 143 (2015).
- [10] S. Hoang, L. Pinsky, R. Vilalta, and J. Jakubek, in *J. Physics: Conference Series* (2012), vol. 396, p. 022023.
- [11] M. Kroupa, A. Bahadori, T. Campbell-Ricketts, A. Empl, S. M. Hoang, J. Idarraga-Munoz, R. Rios, E. Semones, N. Stoffle, L. Tlustos, et al., *A semiconductor radiation imaging pixel detector for space radiation dosimetry*, *Life sciences in space research* **6**, 69 (2015).
- [12] A. A. Bahadori, E. S. Semones, R. Gaza, M. Kroupa, R. R. Rios, N. N. Stoffle, T. Campbell-Ricketts, L. A. Pinsky, and D. Turecek, Tech. Rep. (2015).
- [13] U. Fano, *Penetration of Protons, Alpha Particles, and Mesons*, *Annual Review of Nuclear and Particle Science* **13**, 1 (1963).
- [14] NRC, *National Research Council - Committee on Nuclear Science: Studies in penetration of charged particles in matter*, **1133** (1964).
- [15] J. F. Ziegler, *Handbook of Stopping Cross Sections for Energetic Ions in All Elements*, vol. 5 (Pergamon, New York, NY, 1980).
- [16] R. M. Sternheimer, *Density Effect for the Ionizing Loss of Charged Particles in Various Substances*, *Phys. Rev. B* **26**, 6067 (1982).
- [17] E. Fermi, *The Ionization Loss of Energy in Gases and in Condensed Materials*, *Phys. Rev.* **57**, 485 (1940).
- [18] R. M. Sternheimer, *Range Straggling of Charged Particles in Be, C, Al, Cu, Pb, and Air*, *Phys. Rev.* **117**, 485 (1960).
- [19] R. M. Sternheimer, *Density Effect for the Ionization Loss of Charged Particles*, *Phys. Rev.* **145**, 247 (1966).
- [20] A. Crispin and G. N. Fowler, *Density Effect in the Ionization Energy Loss of Fast Charged Particles in Matter*, *Rev. Mod. Phys.* **42**, 290 (1970).
- [21] J. F. Ziegler, M. D. Zeigler, and J. P. Biersack, *SRIM – The Stopping and Range of Ions in Matter*, *Nuclear Instruments and Methods in Physics Research, Section B: Beam Interactions with Materials and Atoms* **268**, 1818 (2010).
- [22] R. Cabrera-Trujillo, J. R. Sabin, Y. Öhrn, and E. Deumens, *Case for projectile kinetic energy gain in stopping power studies*, *Int. J. Quant. Chem.* **94**, 215 (2003).
- [23] C. Zeitlin, L. Heilbronn, J. Miller, S. E. Rademacher, T. Borak, T. R. Carter, K. A. Frankel, W. Schimmerling, and C. E. Stronach, *Heavy fragment production cross sections from 1.05 GeV/nucleon ^{56}Fe in C, Al, Cu, Pb, and CH_2 targets*, *Phys. Rev. C* **56**, 388 (1997).
- [24] A. S. Lodhi and D. Powers, *Energy loss of α particles in gaseous C-H and C-H-F compounds*, *Phys. Rev. A* **10**, 2131 (1974).
- [25] R. Kreutz, W. Neuwirth, and W. Pietsch, *Analysis of electronic stopping cross sections of organic molecules*, *Phys. Rev. A* **22**, 2606 (1980).
- [26] D. Powers, *Influence of molecular structure on stopping power of chemical species for helium(+) ions from a low-energy particle*

- accelerator*, Accounts of Chemical Research **13**, 433 (1980).
- [27] G. Both, R. Krotz, K. Lohmer, and W. Neuwirth, *Density dependence of stopping cross sections measured in liquid ethane*, Phys. Rev. A **28**, 3212 (1983).
- [28] K. Niita, T. Sato, H. Iwase, H. Nose, H. Nakashima, and L. Sihver, *Phits – a particle and heavy ion transport code system*, Radiation measurements **41**, 1080 (2006).
- [29] P. M. O’Neill, *Badhwar-O’Neill galactic cosmic ray flux model revised*, IEEE Trans. Nuc. Sci **57**, 3148 (2010).
- [30] T. W. Armstrong and K. C. Chandler, *Stopping powers and ranges for muons, charged pions, protons, and heavy ions*, Nuclear Instruments and Methods **113**, 313 (1973).
- [31] T. W. Armstrong and K. C. Chandler, *SPAR, a FORTRAN program for computing stopping powers and ranges for muons, charged pions, protons, and heavy ions*, ORNL-4869, Oak Ridge National Laboratory (1973).
- [32] C. Zeitlin, S. Guetersloh, L. Heilbronn, J. Miller, A. Fukumura, Y. Iwata, and T. Murakami, *Fragmentation cross sections of 290 and 400 MeV/nucleon C 12 beams on elemental targets*, Phys. Rev. C **76**, 014911 (2007).
- [33] C. Zeitlin, S. Guetersloh, L. Heilbronn, J. Miller, A. Fukumura, Y. Iwata, T. Murakami, L. Sihver, and D. Mancusi, *Fragmentation cross sections of medium-energy Cl 35, Ar 40, and Ti 48 beams on elemental targets*, Phys. Rev. C **77**, 034605 (2008).
- [34] T. T. Böhlen, F. Cerutti, M. P. W. Chin, A. Fassò, A. Ferrari, P. G. Ortega, A. Mairani, P. R. Sala, G. Smirnov, and V. Vlachoudis, *The FLUKA code: developments and challenges for high energy and medical applications*, Nuclear Data Sheets **120**, 211 (2014).
- [35] A. Ferrari, P. R. Sala, A. Fassò, and J. Ranft, Tech. Rep. (2005).
- [36] Athreya, K. B., *Bootstrap of the Mean in the Infinite Variance Case*, Ann. Statist. **15**, 724 (1987).
- [37] M. Durante and F. A. Cucinotta, *Heavy ion carcinogenesis and human space exploration*, Nature Reviews Cancer **8**, 465 (2008).
- [38] C. N. Knott, S. Albergo, Z. Caccia, C.-X. Chen, S. Costa, H. J. Crawford, M. Cronqvist, J. Engelage, P. Ferrando, R. Fonte, et al., *Interactions of relativistic neon to nickel projectiles in hydrogen, elemental production cross sections*, Phys. Rev. C **53**, 347 (1996).
- [39] C. Zeitlin, S. Guetersloh, L. Heilbronn, and J. Miller, *Shielding and fragmentation studies*, Radiat. Prot. Dosim. **116**, 123 (2005).
- [40] C. Zeitlin, L. Sihver, C. La Tessa, D. Mancusi, L. Heilbronn, J. Miller, and S. B. Guetersloh, *Comparisons of fragmentation spectra using 1GeV/amu 56 Fe data and the PHITS model*, Radiation Measurements **43**, 1242 (2008).
- [41] ICRP, Tech. Rep. (1991).
- [42] T. C. Slaba, S. R. Blattnig, J. W. Norbury, A. Rusek, C. La Tessa, and S. A. Walker, Tech. Rep. (2015).
- [43] E. Elmore, X.-Y. Lao, R. Kapadia, M. Swete, and J. L. Redpath, *Neoplastic Transformation In Vitro by Mixed Beams of High-Energy Iron Ions and Protons*, Radiation Research **176**, 291 (2011).
- [44] R. J. Fry, *Radiation Protection Dosimetry*, vol. 100 (Oak Ridge TN 378308026, USA, 2002).